Enhanced nonlinear frequency conversion and Purcell enhancement at exceptional points

Adi Pick,[1] Zin Lin,[2] Weiliang Jin,[3] and Alejandro W. Rodriguez[3]
[1]*Department of Physics, Harvard University, Cambridge, Massachusetts 02138, USA*
[2]*John A. Paulson School of Engineering and Applied Sciences, Harvard University, Cambridge, Massachusetts 02138, USA*
[3]*Department of Electrical Engineering, Princeton University, Princeton, New Jersey 08544, USA*
(Received 21 May 2017; published 26 December 2017)

Exceptional points (EPs) were recently predicted to modify the spontaneous emission rate or Purcell factor of narrow-band emitters embedded in resonant cavities. We demonstrate that EPs can have an even greater impact on nonlinear optical processes like frequency conversion by deriving a general formula quantifying radiative emission from a subwavelength emitter in the vicinity of a triply resonant $\chi^{(2)}$ cavity that supports an EP near the emission frequency and a bright mode at the second harmonic. We show that the resulting frequency up-conversion process can be enhanced by up to two orders of magnitude compared to nondegenerate scenarios and that, in contrast to the recently predicted spontaneous-emission enhancements, nonlinear EP enhancements can persist even when considering spatial distributions of broadband emitters, provided that the cavity satisfies special nonlinear selection rules. This is demonstrated via a two-dimensional proof-of-concept PhC designed to partially fulfill the various criteria needed to approach the derived bounds on the maximum achievable up-conversion efficiencies. Our predictions suggest an indirect but practically relevant route to experimentally observe the impact of EPs on spontaneous emission, with implications to quantum information science.

DOI: 10.1103/PhysRevB.96.224303

I. INTRODUCTION

The change in radiative emission experienced by a subwavelength particle near a resonant environment is typically characterized by the well-known Purcell factor [1,2]. Recently, we presented a generalization of Purcell enhancement that applies to situations involving exceptional points (EPs) [3,4]—spectral singularities in non-Hermitian systems where two or more eigenvectors and their corresponding complex eigenvalues coalesce, leading to a nondiagonalizable, defective Hamiltonian. EPs are attended by a slew of intriguing physical effects [5,6] and have been studied in various contexts, including lasers, atomic and molecular systems [7,8], photonic crystals [4,9,10], parity-time symmetric lattices [11–23], optomechanical resonators [24–26], and sensing [27,28]. An important but little explored property of EPs related to light-matter interactions is their ability to modify and enhance the spontaneous emission rate of dipolar emitters, characterized by the local density of states (LDOS) [3,4]. The key to enhancing the LDOS at an EP is to exploit the intricate physics arising from the coalescence of dark and bright (leaky) resonances. Featuring infinite lifetimes and vanishing decay rates, dark modes are by definition generally inaccessible to external coupling. Consequently, an emitter on resonance with a dark mode cannot radiate unless it is also coupled to a leaky resonance. Such a shared resonance underlies the EP enhancements described recently in Refs. [3,4], which showed that the LDOS at an EP exhibits a narrowed, squared Lorentzian line shape whose peak is four times larger than the maximum achievable LDOS of a single resonance. More generally, for an EP of order n, the maximum enhancement factor scales as $\sqrt{n^3}$ [4]. Although this effect makes it possible to enhance (albeit modestly) monochromatic emission near the EP resonance, the existence of a sum rule [29] which forces the frequency-integrated LDOS to be conserved prohibits any enhancement in the case of broadband emitters (e.g., fluorescent molecules).

In this paper, we exploit a coupled-mode theory framework to demonstrate that EPs can have broader and dramatic implications on nonlinear optical processes. In particular, we study radiative emission from a subwavelength emitter, e.g., spontaneous emission from atoms or radiation from classical antennas, that is embedded in a triply resonant nonlinear $\chi^{(2)}$ cavity supporting an EP at the emission frequency along with a second-harmonic resonance, and show that the EP can greatly enhance the resulting frequency up-conversion. The efficiency of such a second-harmonic generation (SHG) process depends strongly on the lifetimes and degree of confinement of the cavity modes [30], which we characterize by deriving a closed-form, analytical formula for the nonlinear Purcell enhancement: the emission rate at $2\omega_e$ from a dipole current source oscillating at ω_e compared to its emission in a bulk medium. Specifically, we provide emission bounds for monochromatic and broadband emitters, showing that the up-conversion rate at the EP can be more than two orders of magnitude larger than that of a single-mode cavity, depending on the position of the emitter and on complicated but designable modal selection rules. We complement our analytical predictions with a concrete physical example—a two-dimensional (2D) PhC slab that partially fulfills all of the aforementioned criteria—and show that EPs can enhance emission from both isolated and spatial distributions of emitters. In combination with recently proposed inverse designs for enhancing nonlinear interactions [4,31], the expected EP enhancements could result in several orders of magnitude larger frequency-conversion efficiencies.

Second-harmonic generation (SHG) is a well-studied process in which light at a frequency ω is converted to 2ω via a $\chi^{(2)}$ nonlinearity [30]. While this effect is typically weak in bulk media [30], it can be greatly enhanced in cavities that confine light both temporally (long decay times) and spatially (small mode volumes). In fact, there has been much interest in designing multiresonant cavities capable of lowering the power requirements of such devices, which are typically

 ©2017 American Physical Society

excited with externally incident light (e.g., from laser sources). While EPs have only been shown to increase the LDOS of cavities (and not their scattering efficiency), one problem which motivates us to explore their impact on nonlinear optics is the closely related challenge of achieving on-chip high-efficiency visible-to-telecom frequency conversion from quantum emitters, a problem of practical value to applications in quantum information science [32]. While there are many relevant nonlinear processes (e.g., two-photon absorption and four-wave mixing) to consider in that context, here we explore the simple but illustrative SHG scheme described above, in which spontaneous emission from an emitter embedded in a triply resonant cavity is up-converted and enhanced due to the presence of an EP at the emission wavelength. Although the design of such a cavity is made difficult by the relatively large number of requirements that must be satisfied if one is to observe significant enhancements, including stringent frequency- and phase-matching criteria [33,34], the creation of an EP at the fundamental wavelength, and special nonlinear modal selection rules (described below), we show that these design challenges can be overcome by application of recently developed inverse-design techniques [31].

II. COUPLED-MODE ANALYSIS

To begin with, consider a generic triply resonant cavity system, depicted schematically in Fig. 1, involving a twofold degeneracy (a_1,b_1) of dark and bright modes at ω_1 and a single mode a_2 at ω_2. Such a system is well described by the following coupled-mode equations (CMEs) [33]:

$$\dot{a}_1 = i\omega_1 a_1 + i\kappa b_1 - \beta_1 a_2 a_1^* - \beta_2 a_2 b_1^* + s_a(t), \quad (1)$$

$$\dot{b}_1 = (i\omega_1 - \gamma_1) b_1 + i\kappa a_1 - \beta_2 a_2 a_1^* - \beta_3 a_2 b_1^* + s_b(t), \quad (2)$$

$$\dot{a}_2 = (i\omega_2 - \gamma_2) a_2 - \beta_1 a_1^2 - \beta_3 b_1^2 - \beta_2 a_1 b_1. \quad (3)$$

Mode a_1 is dark while b_1 and a_2 have decay rates γ_1 and γ_2, respectively. The two degenerate modes are coupled to one another via a linear coefficient κ and nonlinearly coupled to a_2 by a parametric $\chi^{(2)}$ process characterized by mode-overlap coefficients [30,33],

$$\beta_{ij} = \frac{i\omega_1 \int \chi^{(2)} E_2^* E_i E_j d\mathbf{r}}{\sqrt{\int \epsilon_r |E_2|^2 d\mathbf{r}} \sqrt{\int \epsilon_r |E_i|^2 d\mathbf{r}} \sqrt{\int \epsilon_r |E_j|^2 d\mathbf{r}}}, \quad (4)$$

which are defined in terms of the linear cavity electric fields, $E_{\{a,b,2\}}$, corresponding to modes a_1, b_1, and a_2, with $i,j \in \{a,b\}$ and $\beta_{1,2,3} \equiv \{\beta_{aa},\beta_{ab},\beta_{bb}\}$. Note that while β_1 and β_2 involve up-conversion initiated by *either* the dark or bright mode, respectively, β_3 involves both. We focus on emission from a dipolar emitter embedded within the cavity at some position $\mathbf{r}$, represented by the input terms $s_{a,b}(t) = c_{a,b} s(t)$, where the coefficients $c_{a,b} = \frac{1}{\sqrt{V_{a,b}}} = \epsilon_r(\mathbf{r})|E_{a,b}(\mathbf{r})|/(\sqrt{\int d\mathbf{r}\, \epsilon_r |E_{a,b}|^2})$ represent coupling constants which are inversely proportional to the corresponding effective mode volumes, and $s(t) = \int_{-\infty}^{\infty} d\omega \frac{\sqrt{\gamma_e}}{\gamma_e + i(\omega-\omega_e)} e^{i\omega t}$ is a pulse described by a temporal Lorentzian profile of frequency ω_e and decay rate γ_e, and whose Fourier amplitude $s(\omega)$ is normalized so that the integrated power $\int d\omega\, P_e(\omega) = \pi$, with

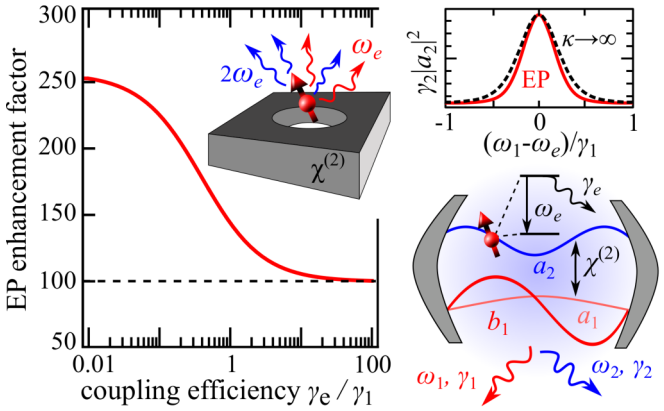

FIG. 1. Schematic of a dipolar Lorentzian emitter of frequecy ω_e and decay rate γ_e embedded in a triply resonant $\chi^{(2)}$ nonlinear cavity supporting an exceptional point (EP). The cavity consists of two degenerate resonances (a_1,b_1) at ω_1, one dark and one bright with decay rate γ_1, that are linearly coupled to one another with coupling rate κ and nonlinearly coupled to a harmonic mode of frequency $\omega_2 = 2\omega_1$ and decay rate γ_2 by the $\chi^{(2)}$ nonlinearity. The spectrum of the cavity consists of two fundamental normal modes $\omega_\pm = \omega_1 \pm \sqrt{\kappa^2 - \gamma_1^2/4}$ of the same effective decay rate $\gamma_1/2$. An EP is formed when $\kappa = \gamma_1/2$, leading to enhanced emission at ω_2 compared to emission in the limit $\kappa \to \infty$ of two far-apart resonances (assuming resonant excitation $\omega_e = \omega_\pm$ of a single normal mode). The main plot shows the largest achievable nonlinear EP enhancement factor, the ratio of the second-harmonic emission rate $P_2 = \gamma_2|a_2|^2$ at the EP to that of the single-mode limit [(10)], as a function of the coupling efficiency $\zeta = \gamma_e/\gamma_1$. The inset (top right) shows P_2 from a monochromatic emitter ($\gamma_e \to 0$) as a function of cavity detuning $\frac{(\omega_e-\omega_1)}{\gamma_1}$, in both the EP (solid) and single-mode (dashed) regimes. For convenience, both emission rates have been normalized.

$P_e(\omega) = |s(\omega)|^2$. Below, we focus on a scenario in which the dipole couples exclusively to the dark mode, such that $c_b = 0$, and consider the consequences of the spectral degeneracy on the emitter's radiation spectrum, given by $P_1(\omega) = \gamma_1|b_1(\omega)|^2$ and $P_2(\omega) = \gamma_2|a_2(\omega)|^2$. We begin with a brief review of the familiar linear Purcell factor ($\beta = 0$), derived for cavities which are well described by a sum of simple Lorentzians, followed by an analysis of the expected modifications arising in the presence of EPs. Finally, we consider the ramifications of EPs on the up-conversion rate (or nonlinear Purcell factor) for finite $\beta > 0$.

III. LINEAR PURCELL ENHANCEMENT

The Purcell factor associated with an emitter which is resonantly coupled to a single-mode cavity of decay rate γ and mode volume V is defined as the ratio of the power radiating from the cavity P_{cav} to that in free space P_{vac} [1,35]. In the case of the Lorentzian emitter above, the enhancement is given by

$$F_P = \frac{P_{\text{cav}}}{P_{\text{vac}}} = \frac{\int_\infty^\infty d\omega \frac{2\gamma}{(\omega-\omega_e)^2+\gamma^2} P_e(\omega)}{V \int_{-\infty}^\infty d\omega \frac{3\omega^2}{\pi^2 c^3} P_e(\omega)} = \frac{3\pi c^3}{\omega_e^2 V(\gamma+\gamma_e)}. \quad (5)$$

This well-known result shows that in order for F_P to be large, the system needs to be in the so-called "bad cavity" or "weak emitter" regime of $\gamma_e \ll \gamma$.

Because the spectrum of a cavity is altered at an EP [3,4,8], one naturally expects some modification to F_P. To illustrate this, we analyze the radiation spectrum of the emitter in the linear regime $\beta = 0$, in which case the source can only couple to the fundamental modes. Solving the CMEs in this regime, one finds that when $\kappa \geqslant \gamma_1/2$, the spectrum $P_1(\omega) = \frac{\gamma_1\kappa^2|c_a|^2}{[\kappa^2-(\omega-\omega_1)^2]^2+\gamma_1^2(\omega-\omega_1)^2} P_e(\omega)$, corresponding to a doubly resonant cavity described by normal modes of frequencies $\omega_\pm = \omega_1 \pm \sqrt{\kappa^2 - \gamma_1^2/4}$ and equal decay rates $\gamma_1/2$. Notably, the normal modes coalesce at $\kappa_{\rm EP} = \gamma_1/2$, forming an EP of complex frequency $\omega_1 - i\gamma_1/2$ which results in the modified spectrum,

$$P_1^{\rm EP}(\omega) = \frac{2|c_a|^2\left(\frac{\gamma_1}{2}\right)^3}{\left[\left(\frac{\gamma_1}{2}\right)^2 + (\omega-\omega_1)^2\right]^2} P_e(\omega), \tag{6}$$

corresponding to a squared Lorentzian of frequency ω_1 and bandwidth $\gamma_1/2$. In the limit $\kappa \to \infty$ of two strongly coupled resonances, the spectrum is well described by a sum of Lorentzians,

$$P_1^{\infty}(\omega) \approx \sum_{\pm} \frac{\frac{\gamma_1}{2}\left|\frac{c_a}{\sqrt{2}}\right|^2}{\left(\frac{\gamma_1}{2}\right)^2 + (\omega-\omega_\pm)^2} P_e(\omega), \tag{7}$$

centered at far-apart frequencies $|\omega_\pm| \gg \omega_1$ and having the same bandwidth $\gamma_1/2$ but smaller amplitudes $c_\infty = c_a/\sqrt{2}$ (or alternatively, larger effective mode volumes) compared to the isolated Lorentzians at κ_∞ (or single-mode regime). Ensuring that the emission is resonant with at least one of the normal modes by setting $\omega_e = \omega_\pm$, and defining the coupling efficiency $\zeta = \gamma_e/\gamma_1$, one obtains the following EP enhancement factor:

$$\mathcal{F}_1(\zeta) = \frac{\int d\omega\, P_1^{\rm EP}(\omega)}{\int d\omega\, P_1^{\infty}(\omega)} = \frac{2(2+\zeta)}{1+\zeta}. \tag{8}$$

Note that this figure of merit quantifies enhancements relative to the typical Purcell factor of (5), with the actual Purcell enhancement at the EP (the emission in the cavity relative to that in vacuum) given by the product $\mathcal{F} \times F_P$.

It follows that in the limit $\gamma_e \to 0$ of a monochromatic emitter, the emission rate at the EP is four times greater than the corresponding rate in the single-mode regime, with $\mathcal{F}_1(\zeta \to 0) = \frac{P_1^{\rm EP}(\omega_1)}{P_1^{\infty}(\omega_\pm)} = \frac{4|c_a|^2/\gamma_1}{2|c_\infty|^2/\gamma_1} = 4$. This result was recently derived in Ref. [3] by exploiting a perturbative expansion of the Maxwell Green's function based on Jordan eigenvectors but, as shown, also follows from the coupled-mode picture. Unfortunately, the larger peak emission at the EP is precisely compensated by a narrowing of the cavity spectrum, the consequence of a general sum rule [29] derived from causality which constrains the frequency-integrated LDOS of any passive system to be conserved, thus ensuring that the cavity spectra above satisfy:

$$\int_{-\infty}^{\infty} d\omega\, \frac{P_1^{\rm EP}(\omega) - P_1^{\infty}(\omega)}{P_e(\omega)} = 0. \tag{9}$$

Consequently, $\mathcal{F}_1$ decreases as the bandwidth of the emitter increases, with $\mathcal{F}_1(\zeta \to \infty) \to 2$ in the "good cavity" limit of a broadband emitter. (Note that while a factor of 2 larger emission technically constitutes enhancement, this is merely an artifact of the lack of degeneracy at κ_∞, with the Lorentzian emitter coupling to a single rather than two modes.) As we show below, such a tradeoff between enhancement and bandwidth is not nearly as prohibitive in the case of finite $\beta > 0$, enabling orders-of-magnitude larger up-conversion rates from sources with bandwidths larger than that of the cavity.

We remark that since the normal modes of the cavity exhibit the same asymptotic decay rates at $\kappa_{\rm EP}$ and κ_∞, the predicted EP enhancements derive only from changes in the cavity dynamics (encoded in the modified spectrum). Moreover, while there are many kinds of EPs one could consider (at least in passive systems), the factor of 4 enhancement can only be attained by EPs comprising dark and bright states and sources that couple strictly to the dark mode (resulting in the squared Lorentzian profile). Intuitively, one could argue that such an enhancement arises because, despite the fact that the underlying coupled resonances exhibit the same asymptotic decay rates, the source is in some sense allowed to directly probe the infinite lifetime of the dark mode. From this perspective, one might expect that while the sum rule of Ref. [29] severely limits the extent to which the emitter can probe the dark versus bright mode, such a restriction could be mitigated in situations involving nonlinear processes, by way of which the energy in the cavity can be disproportionally (i.e., nonlinearly) affected by the dark mode.

IV. NONLINEAR PURCELL ENHANCEMENT

To analyze this scenario, we focus on the typical situation of a weakly nonlinear medium, allowing us to exploit the small-signal or nondepletion approximation of negligible down-conversion, and hence to ignore the nonlinear terms (e.g., $\beta_1 a_2 a_1^*$) entering (1) and (2). Moreover, to ensure that the emitter is coupled resonantly to at least one of the normal modes and that the former is frequency matched to the harmonic mode [33] regardless of κ, we let $\omega_e = \omega_\pm$ and $\omega_2 = 2\omega_\pm$, respectively. As before, any enhancement in the up-conversion rate is expressed relative to the equivalent rate obtained in the single-mode limit $\kappa \to \infty$ of far-apart resonances, in which case one recovers the more familiar description of SHG in doubly resonant cavities [33]. The relevant quantity for this SHG process is the "nonlinear" EP enhancement factor,

$$\mathcal{F}_2(\zeta) = \frac{\int d\omega\, P_2^{\rm EP}(\omega)}{\int d\omega\, P_2^{\infty}(\omega)}, \tag{10}$$

which as before depends on the coupling efficiency ζ.

The perturbative nature of the nondepletion regime allows us to express the spectral amplitude $a_2(\omega)$ of the harmonic mode as a simple convolution, $a_2(\omega) = \frac{i\omega_1/2}{i(\omega-\omega_2)+\gamma_2}\int_{-\infty}^{\infty} dq[\beta_1 a_1(\omega)a_1(\omega-q) + \beta_2 b_1(\omega)b_1(\omega-q) + \beta_3 a_1(\omega)b_1(\omega-q)]$, of the linear ($\beta = 0$) cavity modes at the fundamental frequency and hence to obtain a closed-form expression for (10), which is far too complicated to write here but is detailed in the Appendix. We do however find it instructive to provide expressions for the nonlinear enhancements in the asymptotic bad cavity regime of a

monochromatic emitter ($\zeta \to 0$) as well as the good cavity regime of a broadband emitter ($\zeta \to \infty$), given by

$$\mathcal{F}_2(\zeta \to 0) = \frac{16(4\beta_1 - \beta_2)^2 + 64\beta_3^2}{(\beta_1 + \beta_2 + \beta_3)^2}, \tag{11}$$

$$\mathcal{F}_2(\zeta \to \infty) = \frac{4(5\beta_1 - \beta_2)^2 + 16\beta_3^2}{(\beta_1 + \beta_2 + \beta_3)^2}. \tag{12}$$

These expressions depend on the various nonlinear coefficients in a complicated way, illustrating the asymmetric contribution of the different up-conversion processes, with the dark mode taking a more prominent role. In particular, maximizing $\mathcal{F}_2$ with respect to β, we arrive at upper bounds on the monochromatic and broadband enhancement factors of $\mathcal{F}_2(\zeta \to 0) = 256$ and $\mathcal{F}_2(\zeta \to \infty) = 100$, respectively, achieved under finite $\beta_1 \neq 0$ and $\beta_2 = \beta_3 = 0$. Here, in analogy with the linear result, the largest Purcell enhancements are achieved when the emitter radiates directly into the dark mode and when the latter, in turn, is solely responsible for mediating up-conversion. We find that just as in the linear regime, the harmonic emission spectrum exhibits a higher-order, Lorentzian line shape, illustrated in Fig. 1 (top right), which shows the dependence of $P_2(\zeta \to 0)$ on the cavity detuning $\frac{\omega_1 - \omega_e}{\gamma_1}$ in the monochromatic limit, $\gamma_e \to 0$. Evidently, the emission spectrum undergoes significantly less narrowing compared to the linear scenario above, allowing $\int_{-\infty}^{\infty} d\omega \frac{P_2^{\mathrm{EP}}(\omega) - P_2^{\infty}(\omega)}{P_e(\omega)} > 0$. Note that the above expressions are obtained in the limit $\gamma_2 \ll \gamma_1$ of long second-harmonic lifetimes, since larger decay rates tend to weaken nonlinear effects and hence reduce $\mathcal{F}_2$. Figure 1 summarizes the behavior of $\mathcal{F}_2$ with respect to the coupling efficiency ζ, in analogy with (8).

Naively, one might expect from the linear analysis that the fourfold increase in the peak energy at the fundamental frequency (equivalent to a halving of the mode volume) would translate to a 16-fold increase in the up-conversion rate. Instead and surprisingly, underlying the predicted orders-of-magnitude larger emission rates is the fact that the effective reduction in mode volume enabled by the EP has a compounding and enhancing effect on the nonlinear overlap factors. In fact, inspection of the denominators in (11) and (12) and further analysis of the CMEs reveal that at k_∞, the effect of the dark mode on the nonlinear coefficients is diluted and thus mitigated by the coupling of the emitter to the bright mode, resulting in an effective nonlinear single-mode coupling coefficient $\beta_\infty = \frac{\beta_1 + \beta_2 + \beta_3}{2}$ that is reduced with respect to β_1 by a factor of 2. Alternatively, upon inspection of the numerators of (11) and (12), one can surmise that just as in the linear scenario, those radiative processes which are directly probing the *infinitely longer-lived* dark mode are enhanced (albeit disproportionally) with respect to the others.

V. CAVITY DESIGN

We buttress our theoretical predictions by exploring a simple but concrete physical embodiment of our coupled-mode model designed to satisfy the various criteria required to achieve large nonlinear EP enhancements. First, in a physical cavity, the relative coupling of the emitter to the dark and bright modes will depend on its position as well as on the mode profiles, which must be chosen to ensure that it can couple exclusively to the former. Second, the cavity must support an EP at ω_e and a harmonic resonance at $2\omega_e$. Third, the mode profiles must be designed to ensure large β_1 (known as quasiphase matching [33]) and negligible $\beta_2 = \beta_3 = 0$. These spectral conditions and nonlinear selection rules are all embodied in a proof-of-concept 2D PhC structure, depicted in Fig. 2, that was engineered through inverse design [4].

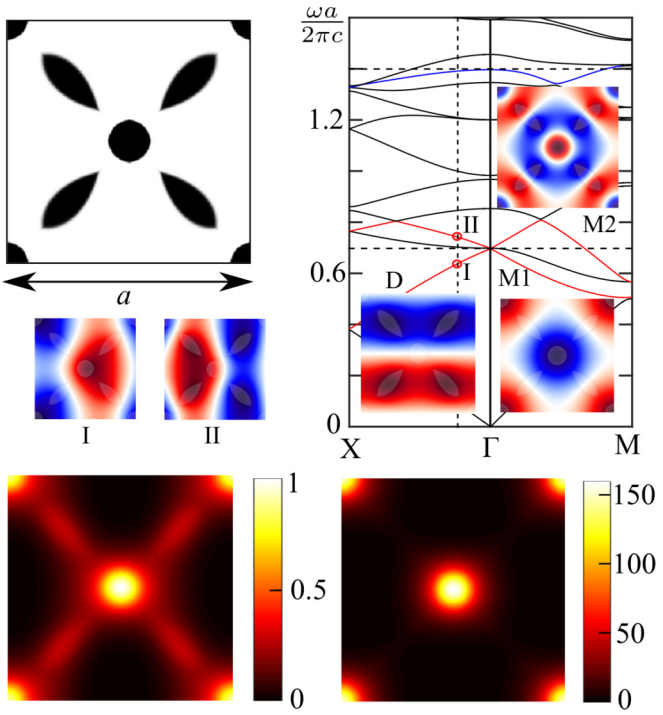

FIG. 2. Inverse-designed 2D square PhC (unit cell). Dark/white regions represent relative permittivities $\epsilon_r = 5.5/1$. The corresponding TM (out-of-plane, scalar electric fields) band structure exhibits a Dirac cone (red bands) centered at ω_1 and a leaky harmonic resonance (blue band) at $\omega_2 = 2\omega_1$. A Dirac degeneracy at Γ is formed by monopolar (M1) and dipolar (D) modes while the second-harmonic resonance is a higher-order monopolar mode (M2), with electric-field profiles shown as insets. Nonhermiticity is introduced by inserting a small amount of dielectric loss along the nodal line of the M1 mode, allowing realization of an EP near ω_1. Also depicted are two nondegenerate modes (I and II) at $k_x a/2\pi = 0.06$ (vertical dashed line in the band diagram), arising from the mixing of the monopole and dipole modes at Γ. The lower panels show the spatially varying emission rate at ω_2 from monochromatic dipole sources distributed throughout the unit cell and oscillating at ω_1, in both the single-mode (left) and EP (right) regimes.

The PhC supports an EP near Γ formed out of a Dirac-point degeneracy [9,31] of dark monopole ($M1$) and bright dipole (D) modes at ω_e, and a bright monopole mode ($M2$) at $2\omega_e$, depicted as insets in Fig. 2. As described in Ref. [4], the band structure of the PhC in the vicinity of the Dirac point can be described by an effective 2×2 Hamiltonian [9],

$$\begin{pmatrix} \omega_1 & v_g k \\ v_g k & \omega_1 + i\gamma_1 \end{pmatrix},$$

where k denotes the Bloch wave number and v_g the group velocity (the slope of the conical dispersion), the product

of which which takes the role of the coupling $\kappa = kv_g$ in our CMEs. Such a system exhibits an EP at $k_{\rm EP} = \gamma_1/2v_g$ and approaches the single-mode or strong-coupling regime at larger $k_\infty \gg k_{\rm EP}$. For computational and conceptual convenience, we introduce nonhermiticity to the system by adding a small amount of absorption ($\mathrm{Im}[\epsilon_r] \neq 0$) along the nodal line of $M1$, which renders the other two modes (D and $M2$) leaky while keeping $M1$ dark. (Note that extending this system to realize a 3D PhC slab leads to a similar effective Hamiltonian.) This judicious choice of mode symmetries ensures that the dipole source couples primarily to the dark mode when it is placed at the center of the unit cell and has the added benefit of realizing $\beta_1 \approx 0.07(\chi^{(2)}/\lambda_1) \gg \beta_2, \beta_3$. Note that, technically, the emission rate at a fixed k is the LDOS per wave number or so-called mutual DOS [36], corresponding to emission from an array of coherent, dipole emitters periodically placed at the center of each unit cell. Hence, angular emission is channeled into the EP modes at $k_{\rm EP}$ and up-converted into the corresponding phase-matched second harmonic mode at $2k_{\rm EP}$. To find the achievable $\mathcal{F}_2$ in this system, we compute the position-dependent coupling constants $c_i(\mathbf{r}) = E_i(\mathbf{r})/\int d\mathbf{r}\, \epsilon_r |E_i(\mathbf{r})|^2$ corresponding to each mode $i = \{M1, D\}$ and solve (1)–(3) to compare the emission rates in the EP and single-mode scenarios. For a dipole located at the center of the unit cell, we obtain monochromatic and broadband enhancement factors of $\mathcal{F}_2(\zeta \to 0) = 160$ and $\mathcal{F}_2(\zeta \to \infty) = 43$, respectively. Note that there is a slight asymmetry in the mode profiles of the far-apart k_∞ resonances, shown in Fig. 2 (insets), indicating that one mode is more localized (and thus has smaller mode volume) than the other. For fairness, the enhancement factor was computed in relation to the more confined of the two modes (labeled I), which explains why $\mathcal{F}_2$ does not reach the bounds obtained above.

Figure 2 also shows the spatially varying, monochromatic up-conversion rate $P_2(\zeta \to 0, \mathbf{r})$ at $k_{\rm EP}$ and k_∞. They differ in at least two important ways: First, the emission rate at the EP depends sensitively on the relative coupling to the dark and bright modes. It reaches its maximum value at the center of the unit cell because away from the center, the source can couple directly to the bright mode, thus diluting the enhancing effect of the dark mode. Second, strong mixing between the dark and bright modes at k_∞ leads to different sets of field profiles, with the k_∞ fields reaching their maximum away from the center. Consequently, the spatially varying $\mathcal{F}_2$ will depend sensitively and in a complicated way on the position of the emitter. To quantify the degree of spatial inhomogeneity or sensitivity to source position, we consider instead the spatially integrated (averaged) enhancement factor, $F_2 = \frac{\int d\mathbf{r}\, P_2^{\rm EP}(\zeta\to 0,\mathbf{r})}{\int d\mathbf{r}\, P_2^{\infty}(\zeta\to 0,\mathbf{r})}$, which captures the net enhancement in the harmonic-emission rate of a uniform distribution of *incoherent* emitters. This quantity is relevant, for instance, to efforts aimed at enhancing large-area fluorescence and lasing in PhCs [37], and will generally depend on the particular structure under consideration. We find that in this geometry, $F_2 = 85$, illustrating the robustness of the nonlinear EP enhancements with respect to the source location. In contrast, the spatially integrated enhancement factor corresponding to monochromatic emission in the linear regime is $F_1 = \frac{\int d\mathbf{r}\, P_1^{\rm EP}(\zeta\to 0,\mathbf{r})}{\int d\mathbf{r}\, P_1^{\infty}(\zeta\to 0,\mathbf{r})} = \frac{2\int d\mathbf{r}\, |c_{\rm M1}|^2}{\int d\mathbf{r}\, |c_{\rm I}|^2} = 2$, showing that just as in the case of a spectrally broadband source $\zeta \to \infty$ [see (8)], there is a sum rule that limits spontaneous emission enhancements from spatially broad sources.

VI. CONCLUDING REMARKS

In summary, we have shown that the efficiency of nonlinear frequency conversion processes can be greatly enhanced in cavities featuring EPs, with ultimate bounds dictated by complicated but tunable modal selection rules favoring interactions mediated by dark states. While luminescence enhancements at EPs in linear media are nullified in the case of broadband emitters, nonlinear Purcell factors can be enhanced by two orders of magnitudes even when the emission bandwidth is much larger than the cavity bandwidth. The ability to exploit larger bandwidths is key to nonlinear applications requiring either fast operational speeds [38] and/or employing good emission sources [39]. In combination with recently demonstrated inverse-designed structures optimized to enhance nonlinear overlaps [31], the proposed EP enhancements could lead to orders-of-magnitude larger nonlinearities and emission efficiencies. We emphasize that our results have general validity and can be applied to a wide range of nonlinear systems, including highly nonlinear midinfrared quantum wells [40], optomechanical resonators [26], and microwave superconducting qubits [41], and that our proof-of-concept geometry is by no means unique. In fact, given a choice of operating frequencies (e.g., microwaves, infrared, or visible wavelengths) and emitters (e.g., qubits, quantum dots, or SiV), there exist many possible nonlinear materials and structures (e.g., ring resonantors or PhC cavities) in which one could demonstrate these effects (especially when aided by inverse design). Finally, we expect that similar or potentially larger enhancements can arise in systems supporting higher-order exceptional points [4,26] or nonlinear processes, e.g., third-harmonic generation, four-wave mixing, and two-photon down-conversion, which have applications in quantum information science.

ACKNOWLEDGMENTS

This work was partially supported by the National Science Foundation under Grant No. DMR-1454836, and by the Princeton Center for Complex Materials, a MRSEC supported by NSF Grant No. DMR 1420541.

A.P., Z.L., and W.J. contributed equally to this work.

APPENDIX: NONLINEAR MODAL AMPLITUDE

To obtain an explicit expression for $a_2(\omega)$, it suffices to Fourier transform (3), in which case one finds the amplitude at the second harmonic in terms of a convolution of the linear modes:

$$a_2(\omega) = \frac{i\omega_1/2}{i(\omega-\omega_2)+\gamma_2}\int_{-\infty}^{\infty} dq[\beta_1 a_1(\omega)a_1(\omega-q) + \beta_3 b_1(\omega)b_1(\omega-q) + \beta_2 a_1(\omega)b_1(\omega-q)], \tag{A1}$$

which can be evaluated to yield a closed-form, analytical solution. Focusing on the EP scenario ($\kappa = \gamma_1/2$) and defining $\Delta = \omega - 2\omega_1$, one obtains

$$\begin{aligned} a_2^{\mathrm{EP}}(\omega) = &-8\pi\gamma_e\{i\beta_2[2c_ac_b(\gamma_1^2\Delta + i\gamma_1^3 + \gamma_1\Delta[4\gamma_e + i(-4\omega_e + 5\omega - 6\omega_1)] + 2\Delta^2(i\gamma_e + \omega_e - \omega + \omega_1)) \\ &+ \gamma_1 c_a^2(2\gamma_1 + i\Delta)[2\gamma_1 + 2\gamma_e + i(-2\omega_e + 3\omega - 4\omega_1)] + \gamma_1\Delta c_b^2(2i\gamma_1 + 2i\gamma_e + 2\omega_e - 3\omega + 4\omega_1)] \\ &+ \beta_1[2\gamma_1 c_a c_b(2\gamma_1 + i\Delta)(2i\gamma_1 + 2i\gamma_e + 2\omega_e - 3\omega + 4\omega_1) \\ &+ c_a^2(8\gamma_1^3 + \gamma_1^2[10\gamma_e + i(-10\omega_e + 21\omega - 32\omega_1)] + 4\gamma_1\Delta(3i\gamma_e + 3\omega_e - 4\omega + 5\omega_1) \\ &- 4\Delta^2[\gamma_e + i(-\omega_e + \omega - \omega_1)]) + \gamma_1^2 c_b^2(-2\gamma_1 - 2\gamma_e + 2i\omega_e - 3i\omega + 4i\omega_1)] \\ &- \beta_3[2\gamma_1\Delta c_a c_b[2\gamma_1 + 2\gamma_e + i(-2\omega_e + 3\omega - 4\omega_1)] + \gamma_1^2 c_a^2[2\gamma_1 + 2\gamma_e + i(-2\omega_e + 3\omega - 4\omega_1)] \\ &+ c_b^2(\gamma_1^2(-2\gamma_e + 2i\omega_e - i\omega) + 4\gamma_1\Delta(-i\gamma_e - \omega_e + \omega - \omega_1) + 4\Delta^2[\gamma_e + i(-\omega_e + \omega - \omega_1)])]\} \\ &/\{[\gamma_1 + i(\omega - 2\omega_1)]^3(-i\gamma_2 + \omega - 2\omega_1)\{\gamma_1 + 2[\gamma_e + i(-\omega_e + \omega - \omega_1)]\}^2(-2i\gamma_e - 2\omega_e + \omega)\}. \end{aligned} \tag{A2}$$

Given this unruly but general expression, we consider two main limiting cases in the main text, corresponding to either a monochromatic ($\gamma_e \to 0, \omega = 2\omega_e$) or broadband ($\gamma_e \gg \gamma_1, \omega_e = \omega_1$) emitter, leading to the equations given in the main text. For comparison, we also consider second-harmonic generation in the $\kappa \to \infty$, in which case the steady-state amplitude is given by

$$a_2^{\infty}(\omega) = \frac{16i\pi\gamma_e\beta_\infty s^\infty}{(-i\gamma_1 + \Delta)(-i\gamma_2 + \Delta)\{\gamma_1 + 2[\gamma_e + i(-\omega_e + \omega - \omega_1)]\}(-2i\gamma_e - 2\omega_e + \omega)}, \tag{A3}$$

where $c_\infty = \frac{1}{\sqrt{2}}(c_a + c_b)$ and $\beta_\infty = \frac{1}{2}(\beta_1 + \beta_2 + \beta_3)$.

[1] E. M. Purcell, H. Torrey, and R. V. Pound, Resonance absorption by nuclear magnetic moments in a solid, Phys. Rev. **69**, 37 (1946).

[2] E. M. Purcell, Spontaneous emission probabilities at radio frequencies, in *Confined Electrons and Photons* (Springer, New York, 1995), p. 839.

[3] A. Pick, B. Zhen, O. D. Miller, C. W. Hsu, F. Hernandez, A. W. Rodriguez, M. Soljačić, and S. G. Johnson, General theory of spontaneous emission near exceptional points, Opt. Express **25**, 12325 (2017).

[4] Z. Lin, A. Pick, M. Lončar, and A. W. Rodriguez, Enhanced Spontaneous Emission at Third-Order Dirac Exceptional Points in Inverse-Designed Photonic Crystals, Phys. Rev. Lett. **117**, 107402 (2016).

[5] N. Moiseyev, *Non-Hermitian Quantum Mechanics* (Cambridge University Press, Cambridge, England, 2011).

[6] T. Kato, *Perturbation Theory for Linear Operators* (Springer-Verlag, Berlin, 1995).

[7] M. V. Berry, Physics of nonhermitian degeneracies, Czech. J. Phys. **54**, 1039 (2004).

[8] W. D. Heiss, The physics of exceptional points, J. Phys. A **45**, 444016 (2012).

[9] B. Zhen, C. W. Hsu, Y. Igarashi, L. Lu, I. Kaminer, A. Pick, S.-L. Chua, J. D. Joannopoulos, and M. Soljacic, Spawning rings of exceptional points out of dirac cones, Nature (London) **525**, 354 (2015).

[10] A. Cerjan, A. Raman, and S. Fan, Exceptional Contours and Band Structure Design in Parity-Time Symmetric Photonic Crystals, Phys. Rev. Lett. **116**, 203902 (2016).

[11] C. M. Bender and S. Boettcher, Real Spectra in Non-Hermitian Hamiltonians Having $\mathcal{PT}$ Symmetry, Phys. Rev. Lett. **80**, 5243 (1998).

[12] Z. Lin, H. Ramezani, T. Eichelkraut, T. Kottos, H. Cao, and D. N. Christodoulides, Unidirectional Invisibility Induced by $\mathcal{PT}$-Symmetric Periodic Structures, Phys. Rev. Lett. **106**, 213901 (2011).

[13] L. Feng, Y.-L. Xu, W. S. Fegadolli, M.-H. Lu, J. B. Oliveira, V. R. Almeida, Y.-F. Chen, and A. Scherer, Experimental demonstration of a unidirectional reflectionless parity-time metamaterial at optical frequencies, Nat. Mater. **12**, 108 (2013).

[14] C. E. Ruter, K. G. Makris, R. El-Ganainy, D. N. Christodoulides, M. Segev, and D. Kip, Observation of parity-time symmetry in optics, Nat. Phys. **6**, 192 (2010).

[15] A. Guo, G. J. Salamo, D. Duchesne, R. Morandotti, M. Volatier-Ravat, V. Aimez, G. A. Siviloglou, and D. N. Christodoulides, Observation of $\mathcal{PT}$-Symmetry Breaking in Complex Optical Potentials, Phys. Rev. Lett. **103**, 093902 (2009).

[16] M. C. Zheng, D. N. Christodoulides, R. Fleischmann, and T. Kottos, $\mathcal{PT}$ optical lattices and universality in beam dynamics, Phys. Rev. A **82**, 010103 (2010).

[17] H. Ramezani, T. Kottos, V. Kovanis, and D. N. Christodoulides, Exceptional-point dynamics in photonic honeycomb lattices with $\mathcal{PT}$ symmetry, Phys. Rev. A **85**, 013818 (2012).

[18] S. Longhi and G. D. Valle, Optical lattices with exceptional points in the continuum, Phys. Rev. A **89**, 052132 (2014).

[19] L. Ge and A. D. Stone, Parity-Time Symmetry Breaking Beyond one Dimension: The Role of Degeneracy, Phys. Rev. X **4**, 031011 (2014).

[20] M. Liertzer, L. Ge, A. Cerjan, A. D. Stone, H. E. Türeci, and S. Rotter, Pump-Induced Exceptional Points in Lasers, Phys. Rev. Lett. **108**, 173901 (2012).

[21] H. Hodaei, M.-A. Miri, M. Heinrich, D. N. Christodoulides, and M. Khajavikhan, Parity-time–symmetric microring lasers, Science **346**, 975 (2014).

[22] L. Feng, Z. J. Wong, R.-M. Ma, Y. Wang, and X. Zhang, Single-mode laser by parity-time symmetry breaking, Science **346**, 972 (2014).

[23] B. Peng, Ş. Özdemir, S. Rotter, H. Yilmaz, M. Liertzer, F. Monifi, C. Bender, F. Nori, and L. Yang, Loss-induced suppression and revival of lasing, Science **346**, 328 (2014).

[24] T. Gao, E. Estrecho, K. Y. Bliokh, T. C. H. Liew, M. D. Fraser, S. Brodbeck, M. Kamp, C. Schneider, S. Hofling, Y. Yamamoto,

F. Nori, Y. S. Kivshar, A. G. Truscott, R. G. Dall, and E. A. Ostrovskaya, Observation of non-hermitian degeneracies in a chaotic exciton-polariton billiard, Nature (London) **526**, 554 (2015).

[25] H. Xu, D. Mason, L. Jiang, and J. Harris, Topological dynamics in an optomechanical system with highly non-degenerate modes, arXiv:1703.07374.

[26] H. Jing, Ş. Özdemir, H. Lü, and F. Nori, High-order exceptional points in optomechanics, Sci. Rep. **7**, 3386 (2017).

[27] H. Hodaei, A. U. Hassan, S. Wittek, H. Garcia-Gracia, R. El-Ganainy, D. N. Christodoulides, and M. Khajavikhan, Enhanced sensitivity at higher-order exceptional points, Nature (London) **548**, 187 (2017).

[28] W. Chen, Ö. Ş. Kaya, G. Zhao, J. Wiersig, and L. Yang, Exceptional points enhance sensing in an optical microcavity, Nature (London) **548**, 192 (2017).

[29] S. M. Barnett and R. Loudon, Sum Rule for Modified Spontaneous Emission Rates, Phys. Rev. Lett. **77**, 2444 (1996).

[30] R. W. Boyd, *Nonlinear Optics* (Academic, CA, San Diego, 1992).

[31] Z. Lin, X. Liang, M. Lončar, S. G. Johnson, and A. W. Rodriguez, Cavity-enhanced second-harmonic generation via nonlinear-overlap optimization, Optica **3**, 233 (2016).

[32] M. W. McCutcheon, D. E. Chang, Y. Zhang, M. D. Lukin, and M. Lončar, Broadband frequency conversion and shaping of single photons emitted from a nonlinear cavity, Opt. Express **17**, 22689 (2009).

[33] A. Rodriguez, M. Soljačić, J. D. Joannopulos, and S. G. Johnson, $\chi^{(2)}$ and $\chi^{(3)}$ harmonic generation at a critical power in inhomogeneous doubly resonant cavities, Opt. Express **15**, 7303 (2007).

[34] Z.-F. Bi, A. W. Rodriguez, H. Hashemi, D. Duchesne, M. Loncar, K.-M. Wang, and S. G. Johnson, High-efficiency second-harmonic generation in doubly-resonant $\chi^{(2)}$ microring resonators, Opt. Express **20**, 7526 (2012).

[35] M. Agio and D. M. Cano, Nano-optics: The purcell factor of nanoresonators, Nat. Photon. **7**, 674 (2013).

[36] R. McPhedran, L. Botten, J. McOrist, A. Asatryan, C. M. de Sterke, and N. Nicorovici, Density of states functions for photonic crystals, Phys. Rev. E **69**, 016609 (2004).

[37] B. Zhen, S.-L. Chua, J. Lee, A. W. Rodriguez, X. Liang, S. G. Johnson, J. D. Joannopoulos, M. Soljačić, and O. Shapira, Enabling enhanced emission and low-threshold lasing of organic molecules using special fano resonances of macroscopic photonic crystals, Proc. Natl. Acad. Sci. USA **110**, 13711 (2013).

[38] M. Soljačić and J. D. Joannopoulos, Enhancement of nonlinear effects using photonic crystals, Nat. Mater. **3**, 211 (2004).

[39] C. Kurtsiefer, S. Mayer, P. Zarda, and H. Weinfurter, Stable Solid-State Source of Single Photons, Phys. Rev. Lett. **85**, 290 (2000).

[40] E. Rosencher, A. Fiore, B. Vinter, V. Berger, Ph. Bois, and J. Nagle, Quantum engineering of optical nonlinearities, Science **271**, 168 (1996).

[41] G. Kirchmair, B. Vlastakis, Z. Leghtas, S. E. Nigg, H. Paik, E. Ginossar, M. Mirrahimi, L. Frunzio, S. M. Girvin, and R. J. Schoelkopf, Observation of quantum state collapse and revival due to the single-photon kerr effect, Nature (London) **495**, 205 (2013).